







TOWARD A LIGHTWEIGHT HIGH-SPEED FIN: STRUCTURAL AND FLUTTER ANALYSIS FOR THICKNESS REDUCTION

Firza Fadlan EKADJ ¹, Wahyu NIRBITO ¹✉, Fadilah HASIM ², Matza Gusto ANDIKA ², Idris Eko PUTRO ², Lilis MARIANI ²

¹Department of Mechanical Engineering, Faculty of Engineering, Universitas Indonesia, Kampus UI Depok, 16424 Depok, Indonesia

²Research Organization of Aeronautics and Space, National Research and Innovation Agency of Indonesia, Jakarta, Indonesia

Article History:

- received 23 May 2025
- accepted 27 October 2025

Abstract. Reducing the mass of supersonic aerodynamic surfaces is a critical challenge in the development of high-speed rockets to further their potential range. This study presents the redesign of a supersonic fin with the primary objective of reducing its thickness from 25 mm. Two designs are investigated, with thicknesses of 10 and 12 mm, respectively, to ensure structural integrity under extreme flight conditions. A comprehensive computational approach is employed, combining static structural analysis, modal analysis, and aeroelastic analysis. Modal analysis is validated through an experimental method using a hammer impulse test for modal frequencies. The 10 mm rocket fin cannot withstand the static load simulated under the flight condition of 15-degree angle of attack, maximum operational flight speed of Mach 3.27, and air density at sea level. The 12 mm thick fin meets the requirements and demonstrates a flutter speed of Mach 11, significantly exceeding the required flutter speed of Mach 3.99. This research highlights the feasibility of substantial weight reduction in supersonic fins without compromising stability, offering a pathway for future advancements in lightweight, high-speed control surfaces.

Keywords: aeroelasticity, modal analysis, finite element analysis, structural design, hammer impact test, supersonic fin.

✉Corresponding author. E-mail: bito@eng.ui.ac.id

Notations

Variables and functions

$[B_{hh}]$ – modal damping matrix;
 b – width of a beam cross-section;
 \bar{c} – reference chord;
 d – height of a beam cross-section;
 E – Young modulus;
 $[K]$ – stiffness matrix;
 $[k_{hh}]$ – modal stiffness matrix;
 $[M]$ – mass matrix;
 $[M_{hh}]$ – modal mass matrix;
 f_a – value obtained by experiment;
 f_c – value obtained by computational analysis;
 I – cross-sectional area moment of inertia;
 l – distance from the clamped end to the free end;
 m – mass;
 $[Q_{hh}^I]$ – modal aerodynamic damping matrix;
 $[Q_{hh}^R]$ – modal aerodynamic stiffness matrix;
 q – dynamic pressure;
 u – speed of a fluid flow;

u_h – modal amplitude vector;
 $\{u\}$ – displacement;
 \ddot{u} – acceleration;
 $\{\ddot{u}\}$ – acceleration;
 $\alpha_i l$ – constant corresponding to an i th mode;
 ρ – density of a fluid;
 $\{\phi\}_i$ – modal eigenvector;
 ω_i – natural frequency on i th mode.

Abbreviations

FEM – Finite Element Method;
 FRF – Frequency Response Function;
 GVT – Ground Vibration Testing;
 NASA – National Aeronautics and Space Administration.

1. Introduction

Reducing the mass of a rocket, provided that structural integrity is maintained, can enhance its flight range. One approach to achieving this is by decreasing the mass of the fins. A straightforward method for modifying an existing

fin design involves reducing its thickness. However, altering this geometric characteristic may affect the fin's susceptibility to flutter. Abou-Amer et al. (2007) stated that it is possible to prevent flutter by increasing the plate thickness. However, Firouz-Abadi and Alavi (2012) have shown that increasing a fin thickness can diminish the stable Mach envelope. Therefore, there is no clear indication of whether reducing a fin thickness would be beneficial in terms of aeroelastic integrity, and a new fin design with an altered magnitude of thickness should be investigated under an aeroelastic analysis.

To enable the numerical aeroelastic calculation of a new fin, a complete flutter model is made, which consists of a structural model and an aerodynamic model (Dinulović et al., 2022). ZONA51 is a linearized aerodynamic small disturbance theory that assumes all interacting lifting surfaces are nearly parallel to the airflow, which is uniform and either steady or undergoing harmonic vibrations (Qiu & Liu, 2021). In the context of modal analysis, a result of a computational analysis using Nastran can be compared to the result of a hammer impact test or an experiment using shaker excitations (Bahari et al., 2021; MSC Software Corporation, 2017; Qaumi & Hashemi, 2023; Wang et al., 2024; Zhang et al., 2019). Compared to the test using shaker excitations, the impulse hammer test has the advantage of cost-effectiveness and shorter time requirements (Reynolds & Pavic, 2000).

This study aims to present a procedure for reducing the thickness of a supersonic fin while ensuring its structural safety under two constraints, i.e., the potential of flutter and a given static load. Firouz-Abadi and Alavi (2012) used a supersonic fin for their study; however, this study differs in that the geometry of the fins used is close to a flat plate, while the paper by Firouz-Abadi and Alavi (2012) used a double wedge fin. This paper presents experimental validation of numerical results using wind tunnel test results and a hammer impulse test, culminating in a discussion of the implications for future advancements in a lightweight, high-speed fin.

This paper will be arranged in the following structure. Following the introduction chapter, the methodology utilized in this research will be elaborated in Section 2. Section 3 presents the experimental data and a comprehensive analysis, comparing the experimental results with numerical ones. The conclusion is depicted in the last section, expressing the close agreement between the results of experiments and numerical simulations, followed by a recommendation for future research.

2. Methodology

The object used as a specimen to reduce the weight is a rocket fin with a mass of 17.2 kg, a thickness of 25 mm, and made up of Al7075 material. This fin, shown in Figure 1, is capable of withstanding an aerodynamic load in a flight with a speed of Mach 3 and a maximum elevation of 28 km. However, the fin was designed for a flight mission

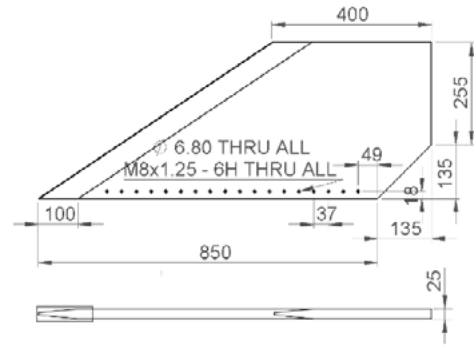


Figure 1. A 25 mm thick supersonic fin (dimensions in mm)

with a predicted maximum speed of Mach 3.27, therefore, this magnitude will be used for this research. A new design with a reduced thickness of 10 mm is chosen as the first design to be investigated since it has one of the smallest thicknesses available for an Al7075 plate on the market.

P-K method has emerged as the most widely adopted approach in aeroelastic engineering; therefore, it is used for the computational flutter analyses (Ju & Qin, 2009). The flutter equation associated with the *p-k* method can be expressed as (Rodden et al., 1979):

$$\left[\begin{array}{c} [M_{hh}]p^2 + \left([B_{hh}] - \frac{1}{4}\rho\bar{c}V[Q'_{hh}]/k \right)p + \\ \left([k_{hh}] - \frac{1}{2}\rho V^2[Q^R_{hh}] \right) \end{array} \right] \{u_h\} = 0, \quad (1)$$

where M_{hh} is the generalized modal mass, B_{hh} is the damping matrix, K_{hh} is the stiffness matrix, Q'_{hh} is the real part of the aerodynamic generalized coefficient matrix, Q^R_{hh} is the imaginary part of the aerodynamic generalized coefficient matrix, ρ is the air density, \bar{c} is the reference chord, k is the reduced frequency, V is velocity, and p is a parameter defined by

$$p^2 = -\frac{V^2}{1+ig}, \quad (2)$$

where g is the artificial structural damping coefficient.

For computational modal and aeroelastic analyses purposes, any design is represented using a finite element model (Cavallo et al., 2017; Bramsiepe et al., 2020). To facilitate the management of aeroelastic models, including highly complex ones, Patran features a dedicated tool called Flightloads (Cestino et al., 2019). This tool enables the creation of flat plate aeromodelling (Hexagon AB, 2021). The computational aeroelastic analyses were performed using the ZONA51 code, which is based on Jones' supersonic theory (Jones, 1948; Chen & Liu, 1985). However, it does not account for the thickness effect (Liu et al., 1994). To attenuate the problem, the authors employed an aerodynamic model that encompasses both lateral sides of the three-dimensional structural model of the fin rather than having an aerodynamic model on a single plane. In the case of flutter predicted at a hypersonic region, validation using a wind tunnel experiment is not

possible in the authors' country since no wind tunnel can produce hypersonic flow. However, the computational method can be used for other hypersonic flutter phenomena documented in experimental studies on flat plates. Two sources are used to provide three flat plate models for flutter analyses to see whether the simulation results are close to the outcome of the experiments (Spain et al., 1995; Xuan et al., 2019). The first model is a flat rudder and was documented to experience flutter at Mach 5. The second and the third models have wing designs and were documented to experience flutter at Mach 18.05 and 17.71, respectively. The first and the second models have blunt edges as their leading edges, which are not characteristic of the supersonic fins in this study. However, the third design has a sharp leading edge, which is present on any of the supersonic fins. The geometric characteristics of all the wind tunnel specimens are represented in Table 1. The assumed properties for these models are a density

of 2800 kg/m^3 and a Young modulus of 73.1 GPa. If the experiment results agree with the outcome of the simulations, the method is, therefore, suitable for the supersonic fins in this study.

The method for determining the new fin design modification based on thickness reduction is summarized in Figure 2. Zhang et al. (2007) used 10% as a criterion point for the relative error between prediction and measurement in their study, where an error below that threshold indicates a good model. However, 5% is used for this study as it is closer to accuracy. The method in Figure 2 starts with selecting a design with one of the smallest possible thicknesses of Al7075 plate available in the market. This design is then examined under a given static load to determine its safety by comparing the maximum stress applied to the yield strength of the material. If it is above, a new design with a small increment of thickness is investigated through the same process. When a design has a maximum

Table 1. Geometry of tested specimens

Model	Root chord	Thickness	Sweep angle	Leading edge shape
1	550 mm	4 mm	38.7°	Blunt
2	10 inches	1/8 inches	70°	Blunt
3	10 inches	1/8 inches	70°	Sharp

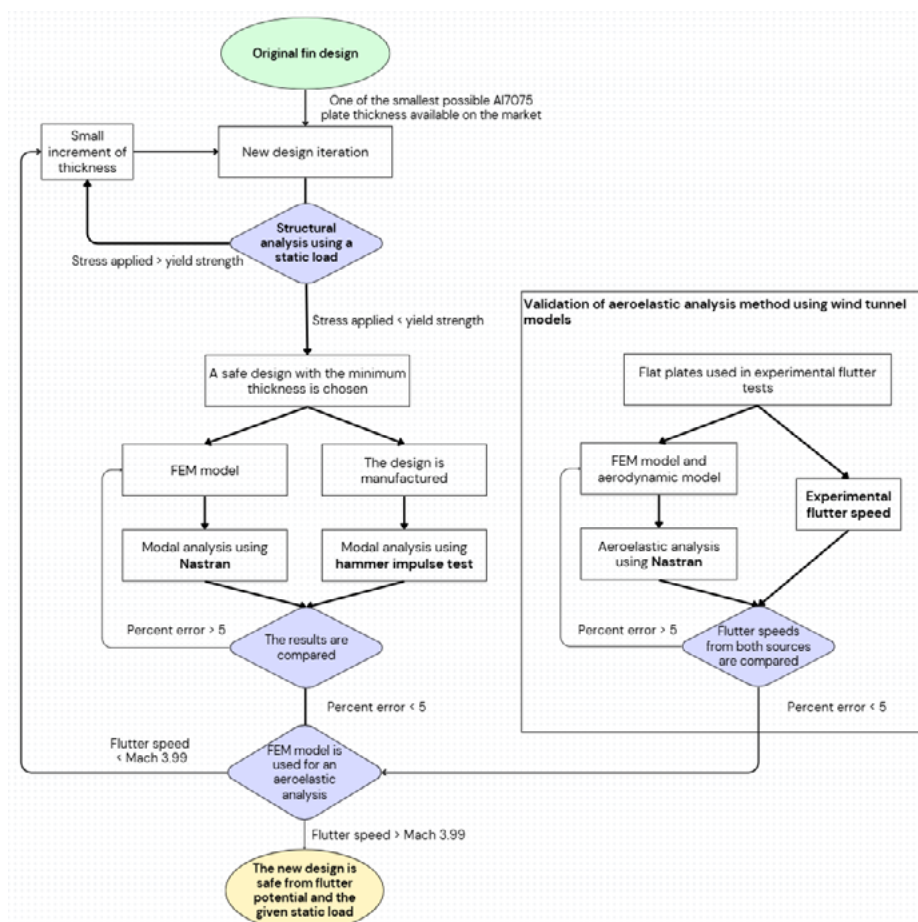


Figure 2. Flow chart of the method used for the rocket fin design modification

stress applied lower than the yield strength under the given static load, it goes through modal analyses using numerical computation and experimentation. This process is needed for the validation of the FEM model used later in the aeroelastic analysis. The natural frequencies resulting from the computational and experimental analyses are compared. If the percent error is above 5, the FEM model needs to be fixed so it can give a more accurate result. If it doesn't reach 5, the FEM model has sufficiently represented the real structure and thus can be used for the aeroelastic analysis.

The aeroelastic analysis method used for this research is validated through the utilization of flat plates used in experimental flutter tests using hypersonic flows. The flutter speeds of the experiments are compared to the flutter speeds obtained by computational aeroelastic analyses on the same plates. If the percent error is above 5, the models used for the computational analyses need to be changed to give more accurate results. If it doesn't reach 5, the computational aeroelastic analysis can then be used on the rocket fin design.

According to Dowell (1972), the panels of space vehicles exposed to a flow shall be designed to be free of flutter at all dynamic pressures up to 1.5 times the local dynamic pressure expected to be encountered at any Mach number within the normal operating flight envelope. Based on a dynamic pressure equation $q = \frac{\rho u^2}{2}$, where ρ is the fluid density and u is the flow speed, if the fluid density is constant, the change in speed that results in a 1.5-fold amplification of the dynamic pressure corresponds to a ratio of 1.22. The minimum flutter speed required, which accounts for the maximum operational flight speed, which is designed to be Mach 3.27, and the required margin of 22%, is Mach 3.99. If the flutter speed resulting from the computational aeroelastic analysis of the new fin design is below this speed, a new iteration of the design with a small increment of thickness is then used back in the structural analysis process using a static load, and the whole required procedure that follows needs to be conducted. If the flutter speed is above Mach 3.99, the new design is acknowledged to be safe from the potential of flutter and the given static load.

3. Results and discussion

In structural contexts, a static load refers to any load applied to a structure that remains constant and does not vary over time. Spaceflight hardware must be engineered to ensure sufficient structural integrity under all anticipated static load conditions (National Aeronautics and Space Administration, 2024). Therefore, a new supersonic fin design with a smaller thickness than the original was put into a computational structural analysis under a given static load. This load arises under the flight condition of a 15-degree angle of attack, a maximum operational flight speed of Mach 3.27, and air density at sea level. The ma-

Table 2. Tensile test results

Specimen	Young Modulus, GPa
1	74
2	71
3	69
4	68
5	72

terial of the design is the same as the previous one, i.e., Al7075. However, a series of tensile tests was conducted to determine the Young modulus of this material. Table 2 shows the results of these tests.

The average of the obtained Young modulus magnitudes is 70.8 GPa, which is used for the analyses. For the properties of the Poisson's ratio and density, this study used values shown in Table 3. Figure 3 shows the contour of the equivalent stress on the structure of the fins after receiving the given static load. The yield strength of the material for a plate with a thickness between 6.35 to 12.67 mm is 462 MPa (The Aluminum Association, Inc., 2009). The figure shows that the equivalent stress on the 10 mm rocket fin design surpasses the yield strength near the rear of the root. This concludes that the 10 mm design cannot handle the given static load. The next design to be put on a similar structural analysis is a design with 12 mm thickness, since 11 mm is not a common thickness available in the market for an Al7075 plate. Figure 4 shows the result of the analysis, and it can be concluded that the equivalent stress on the design doesn't reach the yield strength of the material; therefore, the 12 mm design is chosen as the subject for further analysis. This design has a mass of 51.5% less than the previous design.

The new design features a root chord of 850 mm, a tip chord of 400 mm, and a sweep angle of 33.7°. Eighteen holes are incorporated near the root section to accommodate bolts, which serve as attachment points to the fin's

Table 3. Properties of Al7075 used in this study (He et al., 2015; Shaji et al., 2017)

Property	Value
Poisson's Ratio	0.33
Density (kg/m ³)	2810

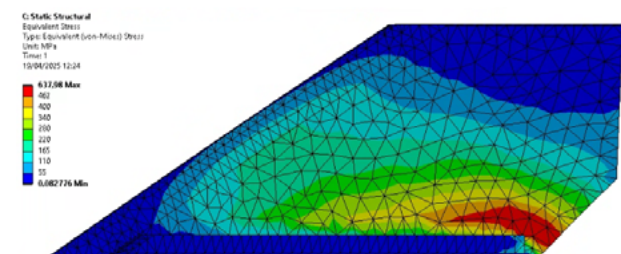


Figure 3. Contour of equivalent stress of a 10 mm rocket fin

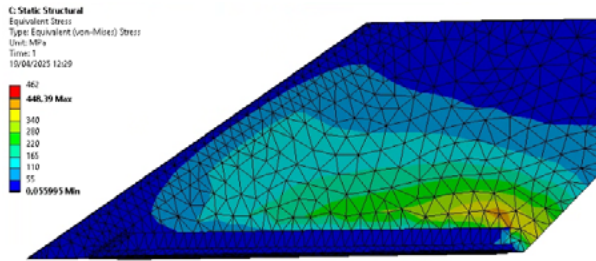


Figure 4. Contour of equivalent stress of a 12 mm rocket fin

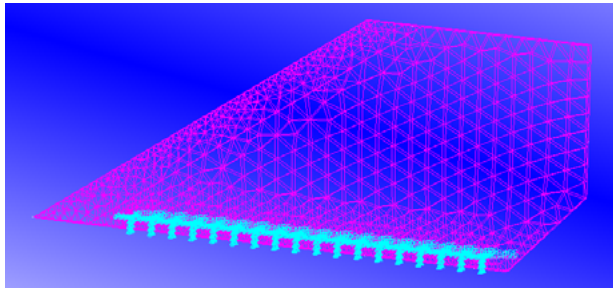


Figure 5. Finite element model of the new fin design along with its constraints

brackets. Figure 5 shows the structural model formed using MSC Patran software. The model consists of 10-node tetrahedral elements. For the modal analysis, all bolt holes are constrained, reflecting their fixed nature when connected to the fin's brackets.

The finite element model of the structure for the simulation is validated using an experiment via modal analysis. The equation of motion for natural frequencies and normal modes in MSC Nastran's normal modes analysis is as follows (Syamsuar et al., 2018):

$$([K] - \omega_i^2 [M])\{\phi\}_i = \{0\}, \quad (3)$$

where $[K]$ is the generalized stiffness matrix, ω_i is the natural frequency, $[M]$ is the generalized mass matrix, and $\{\phi\}_i$ is the modal eigenvector.

Andika et al. (2023a, 2023b) propose an optimized pretest planning strategy for modal testing and ground vibration testing (GVT) of UAVs with high aspect ratio wings, which are highly susceptible to aeroelastic loads. By utilizing finite element models to determine optimal excitation, sensor placement, and support locations, the study employs methods such as MAC, SEAMAC, normalized kinetic energy, and mode participation analysis to enhance measurement accuracy, ensure structural integrity, and improve flight safety. This pretest planning approach is crucial for optimizing set points for impact hammer and accelerometer placement, ultimately leading to more effective and reliable structural dynamic characterization.

Figure 6 shows the setup for the hammer-impulse test, displaying 15 designated impact points on the fin. Figure 7 presents the experimental FRF data, where the colored lines correspond to the measurements obtained from impacts at the designated points. Each peak produced from

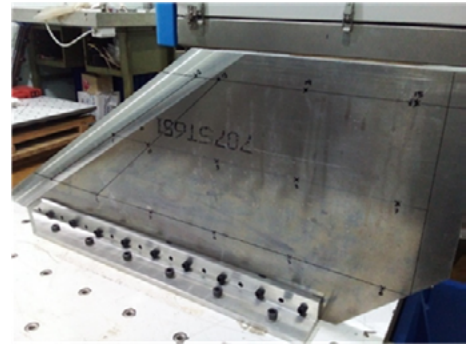


Figure 6. Setup for hammer-impulse test

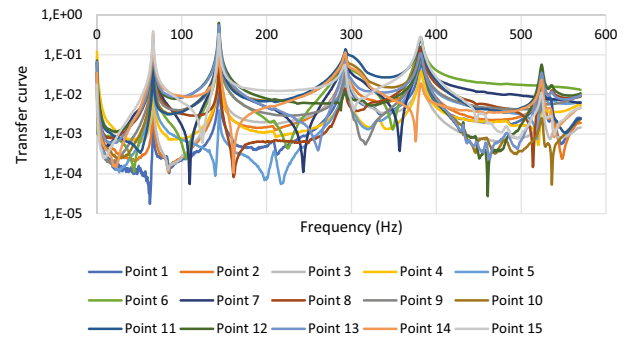


Figure 7. FRF of the hammer impact test

the combination of the lines shows the location of the natural frequency of the specimen.

The results of the modal analysis simulation and the hammer-impulse test are compared in Table 4 along with the percent error values. The calculation for the percent error between the computational and experimental natural frequencies is based on the following equation (Rayer, 2007).

$$\text{Percent error} = \frac{f_c - f_e}{f_e} \times 100, \quad (4)$$

where f_c is the value obtained by computational analysis and f_e is the value obtained by experiment. The percent error values in this study are presented in absolute form. The percent error of each comparison in Table 4 between the results for the first five modes is under 2, indicating good model accuracy. In the case of the original 25 mm thick fin, the natural frequencies for the first five modes are, consecutively, 135.12 Hz, 289.13 Hz, 508.73 Hz, 584.76 Hz, and 758.81 Hz. The mode shapes of the first, the second, the fourth, and the fifth modes are similar to those of the first four modes of the 12 mm thick fin. The percentage change of each natural frequency for the four modes from those of the 25 mm thick fin to those of the 12 mm thick fin is, consecutively, -50.9%, -50.3%, -49.9%, and -49.8%. If one uses a clamp-free beam's natural frequency Equation (5) as an approximation for the 12 mm thick fin's natural frequencies, and uses the moment of inertia for a rectangular cross-section $I = \frac{bd^3}{12}$ the a second approximation, the percentage changes of the natural

Table 4. Comparison of the natural frequencies of the 12 mm thick fin between the experimental result and the computational result

No.	Experimental frequency, Hz	Computational frequency, Hz	Percent Error	Vibration mode
1	66.3	67.4	1.7	1st bending
2	143.8	141.9	1.3	1st torsion
3	293.1	289.8	1.1	2nd torsion
4	381.3	383.1	0.5	2nd bending
5	524.4	523.3	0.2	3rd bending

Table 5. Comparison of the natural frequencies of the models used in flutter experiments

Model	Computational frequency, Hz		Experimental frequency, Hz		Percent Error	
	1 st mode	2 nd mode	1 st mode	2 nd mode	1 st mode	2 nd mode
1	27.55	33.24	25.6	36.7	7.6	9.4
2	9.43	18.04	10	18	5.7	0.2
3	10	19.4	10.5	20.5	4.8	5.4

Table 6. Computational aeroelastic analyses results with comparison to the experimental results

Model	Computational flutter speed	Experimental flutter speed	Percent Error
1	Mach 5.02	Mach 5	0.4
2	Mach 18.06	Mach 18.05	0.1
3	Mach 18.1	Mach 17.71	2.2

frequencies by only changing the thickness of the fin are consistent throughout all the modes, which closely align with the values of the aforementioned calculated percentage changes.

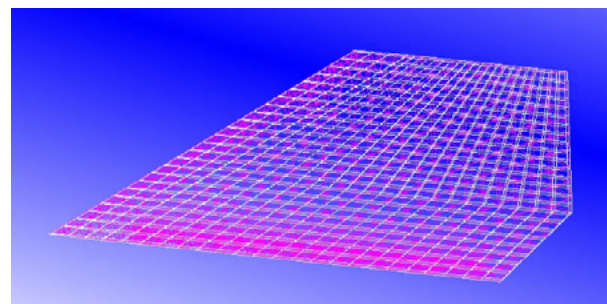
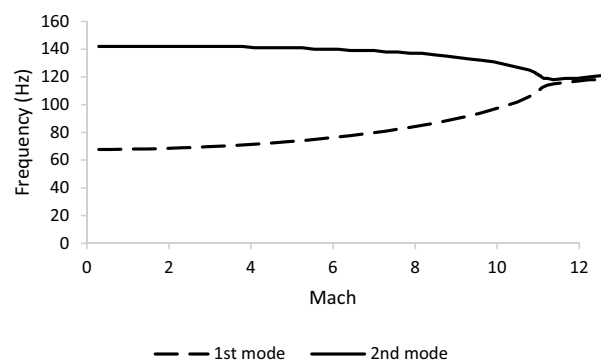
$$\omega_i = (\alpha_i l)^2 \sqrt{\frac{EI}{ml^4}}. \quad (5)$$

Three models tested in flutter experiments were used for computational modal analyses and flutter analyses. Table 5 shows the natural frequencies for the first two modes obtained from computational analyses and literature. The percent errors lie below 10, indicating good model accuracy; therefore, the FEM models can be used for aeroelastic analyses (Zhang et al., 2007).

The results of computational aeroelastic analyses on the three models tested in flutter experiments are summarized in Table 6. The percent errors with respect to the experimental results lie under 5, which gave enough confidence to use the same method for the flutter analysis on the new fin design.

Figure 8 shows the structural model along with the aerodynamic model for the aeroelastic analysis of the 12-mm-thick fin. The aerodynamic model consists of panels that cover both lateral sides of the fin, including the major flat section and the leading edge. As in the modal analysis, the bolt holes are constrained. Figures 9 and 10 show the results of the analysis.

Flutter is an aeroelastic instability that arises when the damping of a particular vibrational mode reduces to zero

**Figure 8.** Structural model and aerodynamic model of the 12-mm thick fin**Figure 9.** Frequency – Mach graph of the thickness-reduced fin

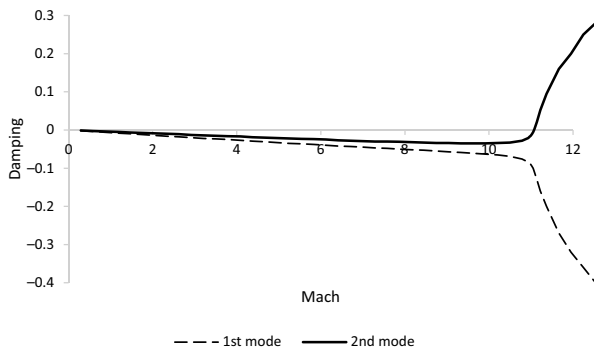


Figure 10. Damping – Mach graph of the thickness-reduced fin

(Hancock et al., 1985). Within the framework of the present analysis, the onset of flutter is identified at a freestream Mach number of 11. At this condition, the modal damping corresponding to the second mode transitions monotonically from a small negative value to zero, signalling the onset of flutter. This transition provides a precise indicator of the point at which dynamic stability is lost. From a safety perspective, this predicted flutter Mach number greatly exceeds the required speed. Specifically, the computed flutter speed is approximately 2.8 times higher than the prescribed design threshold of Mach 3.99. The latter value is obtained by applying a safety factor of 1.22 to the maximum predicted operational speed of Mach 3.27.

4. Conclusions

Analyses for thickness-reduced fin designs have been completed to see whether they meet the structural safety requirements against a given static load and the potential of flutter. After a computational structural analysis using a static load, a new fin design with a thickness of 10 mm fails to meet the aforementioned requirement. However, the 12 mm thick design is considered to be safe under a structural analysis and has an obtained flutter speed 2.8 times higher than the requirement under an aeroelastic analysis; therefore, it is safe from the potential of flutter.

This research also depicts that the numerical results of the modal analysis of the 12 mm thick fin have a close agreement with the experimental results, with margins of error of under 2 percent. In the context of the structural analyses conducted under static loading conditions, the authors have found that the location of maximum equivalent stress for each case is situated near the posterior region of the root. The authors have also found that the results of the computational aeroelastic analyses using models that had previously been subjected to flutter experiments and the aerodynamic models made in a manner described in the study are in close agreement with the experimental data. Further study of this computational-experimental validation approach to a broader range of models is recommended to evaluate the range of utility of the computational method.

The thickness reduction approach has successfully yielded a lighter fin design with the consideration of the aspect of aeroelasticity, thereby offering a viable alternative fin design that has the potential to enhance overall rocket performance. Further research is required to find other alternative methods of reducing the mass of the original fin to see if they would result in a more significant mass reduction.

Funding

This research was supported by RIIM-LPDP Research Program Batch 1 Year 2022 under Grant No. B-808/II.7.5/FR/6/2022 and B-9546/III.1/KS.00.00/6/2022, and Rumah Program with a topic “Optimization of Rocket Components Based on Natural Fiber Composite and Metal under Dynamic Load”.

Author contributions

Firza Fadlan Ekadj wrote the manuscript and did the structural and aeroelastic analyses. Guidance and writing recommendations were given by Wahyu Nirbito as a corresponding author, Fadilah Hasim, and Idris Eko Putro. Matza Andika Gusto gave assessments for methodology and analyses. Lilis Mariani observed the hammer impact test facility and helped with the realization of the research funding.

Disclosure statement

The authors declare that they have no financial interests or personal/professional relationships with the third parties that could be perceived as influencing the work presented in this paper.

References

- Abou-Amer, S., Dahshan, A., & El Nomrossy, M. (2007). Nonlinear panel flutter analysis at high supersonic speed. *Mansoura Engineering Journal*, 32(2). <https://doi.org/10.21608/bfemu.2020.128541>
- Andika, M. G., Moelyadi, M. A., Sasongko, R. A., & Hadi, B. K. (2023a). Finite element assisting for effective ground vibration test planning on very flexible aircraft. *AIP Conference Proceedings*, 2941(1), Article 020044. <https://doi.org/10.1063/5.0181451>
- Andika, M. G., Moelyadi, M. A., Sasongko, R. A., & Hadi, B. K. (2023b). Pretest planning approach for optimal modal testing on high aspect ratio wing structure. *Iranian Journal of Science and Technology, Transactions of Mechanical Engineering*, 47, 1109–1120. <https://doi.org/10.1007/s40997-022-00564-3>
- Bahari, A. R., Yunus, M. A., Rani, M. N. A., Mirza, W. I. I. W. I., Shah, M. A. S. A., & Yahya, Z. (2021). Finite element modelling and updating of a thin plate structure using normal mode analysis. *IOP Conference Series: Materials Science and Engineering*, 1062(1), Article 012059. <https://doi.org/10.1088/1757-899X/1062/1/012059>
- Bramsiepe, K., Voß, A., & Klimmek, T. (2020). Design and sizing of an aeroelastic composite model for a flying wing configuration

- with maneuver, gust, and landing loads. *CEAS Aeronautical Journal*, 11, 677–691.
<https://doi.org/10.1007/s13272-020-00446-x>
- Cavallo, T., Zappino, E., & Carrera, E. (2017). Component-wise vibration analysis of stiffened plates accounting for stiffener modes. *CEAS Aeronautical Journal*, 8, 385–412.
<https://doi.org/10.1007/s13272-017-0244-5>
- Cestino, E., Frulla, G., Spina, M., Catelani, D., & Linari, M. (2019). Numerical simulation and experimental validation of slender wings flutter behaviour. *Proceedings of the Institution of Mechanical Engineers, Part G: Journal of Aerospace Engineering*, 233(16). <https://doi.org/10.1177/0954410019879820>
- Chen, P.-C., & Liu, D. D. (1985). A harmonic gradient method for unsteady supersonic flow calculations. *Journal of Aircraft*, 22(5).
<https://doi.org/10.2514/3.45134>
- Dinulović, M., Rašuo, B., Slavković, A., & Zajić, G. (2022). Flutter analysis of tapered composite fins: Analysis and experiment. *FME Transactions*, 50(3), 576–585. <https://doi.org/10.5937/fme2203576D>
- Dowell, E. H. (1972). Panel flutter. In *NASA Space Vehicle Design Criteria (Structures)*. National Aeronautics and Space Administration.
- Firouz-Abadi, R. D., & Alavi, S. M. (2012). Effect of thickness and angle-of-attack on the aeroelastic stability of supersonic fins. *The Aeronautical Journal*, 116(1182).
<https://doi.org/10.1017/S0001924000007272>
- Hancock, G. J., Wright, J. R., & Simpson, A. (1985). On the teaching of the principles of wing flexure-torsion flutter. *The Aeronautical Journal*, 89(888). <https://doi.org/10.1017/S0001924000015050>
- He, C., Liu, Y., Dong, J., Wang, Q., Wagner, D., & Bathias, C. (2015). Fatigue crack initiation behaviors throughout friction stir welded joints in AA7075-T6 in ultrasonic fatigue. *International Journal of Fatigue*, 81, 171–178.
<https://doi.org/10.1016/j.ijfatigue.2015.07.012>
- Hexagon AB. (2021). *MSC FlightLoads 2021.4 user's guide*. https://help-be.hexagonmi.com/bundle/MSC_FlightLoads_2021.4_User_Guide/raw/resource/enus/MSC_FlightLoads_2021.4_User_Guide.pdf
- Jones, W. P. (1948). *Supersonic theory for oscillating wings of any plan form*. British Aeronautical Research Council R&M 2655.
- Ju, Q., & Qin, S. (2009). New improved g method for flutter solution. *Journal of Aircraft*, 46(6). <https://doi.org/10.2514/1.46328>
- Liu, D. D., Yao, Z. X., Sarhaddi, D., & Chavez, F. (1994). *Piston theory revisited and further applications* (ICAS Paper 94-2.8.4). ICAS.
- MSC Software Corporation. (2017). *Dynamic analysis user's guide*. <https://simcompanion.hexagon.com/customers/s/article/msc-nastran-2018-dynamic-analysis-user-s-guide-doc11514>
- National Aeronautics and Space Administration. (2024). *Loads and structural dynamics requirements for spaceflight hardware*. NASA.
- Qaumi, T., & Hashemi, S. (2023). Experimental and numerical modal analysis of a composite rocket structure. *Aerospace*, 10(10), Article 867. <https://doi.org/10.3390/aerospace10100867>
- Qiu, J., & Liu, C. (2021). Verification and validation of supersonic flutter of rudder model for experiment. In M. S. G. Tsuzuki, R. Y. Takimoto, A. K. Sato, Saka, T., Barari, A., Rahman, R. O. A., & Hung, Y.-T. (Eds.), *Engineering problems – uncertainties, constraints and optimization techniques*. IntechOpen.
<https://doi.org/10.5772/intechopen.98384>
- Rayer, S. (2007). Population forecast accuracy: Does the choice of summary measure of error matter? *Population Research and Policy Review*, 26, 163–184.
<https://doi.org/10.1007/s11113-007-9030-0>
- Reynolds, P., & Pavic, A. (2000). Impulse hammer versus shaker excitation for the modal testing of building floors. *Experimental Techniques*, 24(3), 39–44.
<https://doi.org/10.1111/j.1747-1567.2000.tb00911.x>
- Rodden, W., Harder, R., & Bellinger, E. (1979). *Aeroelastic addition to NASTRAN* (NASA CR-3094). NASA.
- Shaji, B., V. K., A. S., & V. J. (2017). Structural analysis on AI 7075 T-651 shaft. *Journal of Chemical and Pharmaceutical Sciences*, 10(1), 646–648.
- Spain, C. V., Zeiler, T., & Bullock, E., Hodge, J. (1995). A flutter investigation of all-moveable NASP-like wings at hypersonic speeds. In *34th Structures, Structural Dynamics and Materials Conference*. Aerospace Research Central.
<https://doi.org/10.2514/6.1993-1315>
- Syamsuar, S., Sampurno, B., Mahasti, K. M., Pratama, M. B. S., Sasongko, T. W., Kartika, N., Adityo, S., Ivan, M., & Eskayudha, D. B. (2018). Half wing N219 aircraft model clean configuration for flutter test on low speed wind tunnel. *Journal of Physics: Conference Series*, 1005(1), Article 012040.
<https://doi.org/10.1088/1742-6596/1005/1/012040>
- The Aluminum Association, Inc. (2009). *Aluminum standards and data 2009*. The Aluminum Association, Inc.
- Wang, G., Xie, C., Liu, C., & An, C. (2024). Hypersonic flutter analysis based on three-dimensional local piston theory. In *International Forum on Aeroelasticity and Structural Dynamics (IFASD 2024)*. The Hague, The Netherlands.
- Xuan, C., Han, J., Zhang, B., Yun, H., & Chen, X. (2019). Hypersonic flutter and flutter suppression system of a wind tunnel model. *Chinese Journal of Aeronautics*, 32(9), 2121–2132.
<https://doi.org/10.1016/j.cja.2019.02.009>
- Zhang, W., Lv, Z., Diwu, Q., & Zhong, H. (2019). A flutter prediction method with low cost and low risk from test data. *Aerospace Science and Technology*, 86, 542–557.
<https://doi.org/10.1016/j.ast.2019.01.043>
- Zhang, Z., Zhang, W., Zhai, Z. J., & Chen, Q. Y. (2007). Evaluation of various turbulence models in predicting airflow and turbulence in enclosed environments by CFD: Part 2 – comparison with experimental data from literature. *HVAC&R Research*, 13(6), 871–886. <https://doi.org/10.1080/10789669.2007.10391460>